Turbulence and Interactions

Proceedings the TI 2009 Conference

Michel Deville
Thien-Hiep Lê
Pierre Sagaut
(Editors)

Springer

Prof. Michel Deville
EPFL STI IGM LIN
Station 9
1015 Lausanne
Switzerland
E-mail: michel.deville@epfl.ch

Prof. Pierre Sagaut
Institut Jean Le Rond d'Alembert
Université Pierre et Marie Curie
4 Place Jussieu
75252 Paris cedex 5
France

Dr. Thien-Hiep Lê
ONERA
29 Avenue de la Division Leclerc
92322 Chatillon
France

ISBN 978-3-642-14138-6 e-ISBN 978-3-642-14139-3

DOI 10.1007/978-3-642-14139-3

Notes on Numerical Fluid Mechanics
and Multidisciplinary Design ISSN 1612-2909

Library of Congress Control Number: 2010929478

Typeset & Cover Design: Scientific Publishing Services Pvt. Ltd., Chennai, India.

Printed on acid-free paper

5 4 3 2 1 0

springer.com

NNFM Editor Addresses

Prof. Dr. Wolfgang Schröder
(General Editor)
RWTH Aachen
Lehrstuhl für Strömungslehre und
Aerodynamisches Institut
Wüllnerstr. 5a
52062 Aachen
Germany
E-mail: office@aia.rwth-aachen.de

Prof. Dr. Kozo Fujii
Space Transportation Research Division
The Institute of Space
and Astronautical Science
3-1-1, Yoshinodai, Sagamihara
Kanagawa, 229-8510
Japan
E-mail: fujii@flab.eng.isas.jaxa.jp

Dr. Werner Haase
Höhenkirchener Str. 19d
D-85662 Hohenbrunn
Germany
E-mail: office@haa.se

Prof. Dr. Ernst Heinrich Hirschel
(Former General Editor)
Herzog-Heinrich-Weg 6
D-85604 Zorneding
Germany
E-mail: e.h.hirschel@t-online.de

Prof. Dr. Ir. Bendiks Jan Boersma
Chair of Energytechnology
Delft University of Technology
Leeghwaterstraat 44
2628 CA Delft
The Netherlands
E-mail: b.j.boersma@tudelft.nl

Prof. Dr. Michael A. Leschziner
Imperial College of Science
Technology and Medicine
Aeronautics Department
Prince Consort Road
London SW7 2BY
U.K.
E-mail: mike.leschziner@ic.ac.uk

Prof. Dr. Sergio Pirozzoli
Università di Roma "La Sapienza"
Dipartimento di Meccanica e Aeronautica
Via Eudossiana 18
00184, Roma, Italy
E-mail: sergio.pirozzoli@uniroma1.it

Prof. Dr. Jacques Periaux
38, Boulevard de Reuilly
F-75012 Paris
France
E-mail: jperiaux@free.fr

Prof. Dr. Arthur Rizzi
Department of Aeronautics
KTH Royal Institute of Technology
Teknikringen 8
S-10044 Stockholm
Sweden
E-mail: rizzi@aero.kth.se

Dr. Bernard Roux
L3M – IMT La Jetée
Technopole de Chateau-Gombert
F-13451 Marseille Cedex 20
France
E-mail: broux@l3m.univ-mrs.fr

Prof. Dr. Yurii I. Shokin
Siberian Branch of the
Russian Academy of Sciences
Institute of Computational
Technologies
Ac. Lavrentyeva Ave. 6
630090 Novosibirsk
Russia
E-mail: shokin@ict.nsc.ru

Preface

The "Turbulence and Interactions 2009" (TI2009) conference was held in Saint-Luce on the island of La Martinique, France, on May 31-June 5, 2009. The scientific sponsors of the conference were

- DGA
- Ecole Polytechnique Fédérale de Lausanne (EPFL),
- ERCOFTAC : European Research Community on Flow, Turbulence and Combustion,
- Institut Jean Le Rond d'Alembert, Paris,
- ONERA.

This second TI conference was very successful as it attracted 65 researchers from 17 countries. The magnificent venue and the beautiful weather helped the participants to discuss freely and casually, share ideas and projects, and spend very good times all together.

The organisers were fortunate in obtaining the presence of the following invited speakers: L. Fuchs (KTH, Stockholm and Lund University), J. Jimenez (Univ. Politecnica Madrid), C.-H. Moeng (NCAR), A. Scotti (University of North Carolina), L. Shen (Johns Hopkins University) and A.J. Smits (Princeton University). The topics covered by the 62 contributed papers ranged from experimental results through theory to computations. They represent a snapshot of the state-of-the-art in turbulence research. The papers of the conference went through the usual reviewing process and the result is given in this book of Proceedings.

In the present volume, the reader will find the keynote lectures followed by the contributed talks given in alphabetical order of the first author.

The organizers of the conference would like to acknowledge the support of EPFL, Université Pierre et Marie Curie, Paris and ONERA. They express their gratitude for their colleagues of the organizing committee, especially Drs. V. Gleize and M. Terracol, for their help and constant efficiency.

Lausanne, Paris
December 3, 2009

M. O. Deville
T. H. Lê
P. Sagaut

Contents

Some Characteristics of Non-Reacting and Reacting Low Swirl Number Jets

L. Fuchs

Abstract. The paper considers low swirl turbulent number jets. Swirling jets are used to stabilize premixed flames in gas turbines. Normally, the swirl number is large enough to allow vortex break-down and thereby flame stabilization along the upstream edge of the back-flow bubble. With decreasing swirl the vortex-breakdown may disappear altogether. However, it has been found that under certain conditions the flame may be kept at a certain (mean) distance away from the nozzle even without vortex break-down. The mechanism for the flame holding under such conditions is discussed. The discussion is based upon LES results and some experimental data. We discuss also the precession of the central core both under non-reacting and reacting condition. LES and experimental results show that the precession of the central core is normally in the same direction as the swirl. However, for certain range of swirl numbers and at some axial distances one may find precession in the counter direction. The mechanism for this effect is discussed.

L. Fuchs
Linné Flow Centre, Royal Institute of Technology, Stockholm, Sweden
e-mail: lf@mech.kth.se

M. Deville, T.-H. Lê, and P. Sagaut (Eds.): Turbulence and Interactions, NNFM 110, p. 1.
springerlink.com

Inner-Outer Interactions in Wall-Bounded Turbulence

Javier Jiménez

1 Introduction

This paper deals with some of the features that distinguish wall-bounded sheared turbulence from that in free-shear flows. It concerns itself mostly with the largest structures at each wall distance, because they are where energy is fed into the fluctuations, and therefore the ones that differ most between the different flows. Because of the geometric limitations imposed by the wall, the largest scales roughly coincide with the smallest ones in the viscous buffer layer, but the rest of the flow is characterised, as in most turbulent cases, by a wide range of scales.

Wall-bounded turbulence includes pipes, channels and boundary layers. We restrict ourselves to cases with little or no longitudinal pressure gradients, since otherwise the flow tends to separate and resembles the free-shear case. It was in attached wall-bounded flows where turbulence was first studied scientifically [16, 6], but they remain to this day worse understood than homogeneous or free-shear turbulence. That is in part because what is sought in both cases is different. Turbulence is a multiscale phenomenon. Energy resides in the largest eddies, but it cannot be dissipated until it is transferred to the smaller scales for viscosity to act. The classical conceptual framework for that process is the self-similar cascade [35, 28], which assumes that the transfer is local in scale space, with no significant interactions between eddies of very different sizes. The resulting model, although now recognised as only an approximation, describes well the experimental observations in isotropic turbulence, but also in small-scale turbulence in general. A sketch can be found in figure 1(a).

The emphasis in shear flows is not on the transfer of energy, but on its production. Isotropic theory gives no indication of how energy is fed into the cascade. In shear flows, the energy source is the interaction between the mean velocity gradient and the average momentum fluxes carried by the velocity fluctuations [39]. In free-shear

Javier Jiménez
School of Aeronautics, U. Politécnica, 28040 Madrid, Spain
e-mail: jimenez@torroja,dmt.upm.es

M. Deville, T.-H. Lê, and P. Sagaut (Eds.): Turbulence and Interactions, NNFM 110, pp. 3–14.
springerlink.com

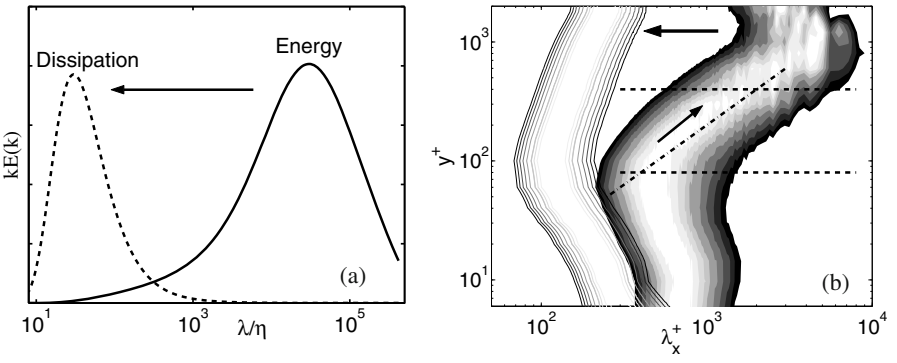

Fig. 1 Spectral energy density, $kE(k)$. (a) In isotropic turbulence, as a function of the isotropic wavelength $\lambda = 2\pi/|k|$. (b) In a turbulent channel [17] with $h^+ = 2000$, plotted as a function of the streamwise wavelength λ_x, and of the wall distance y. Shaded contours are the density of the kinetic energy, $k_x E_{\mathbf{uu}}(k_x)$. Lines are the spectral density of the surrogate dissipation, $\nu k_x E_{\omega\omega}(k_x)$, where ω are the vorticity fluctuations. At each y the lowest contour is 0.86 times the local maximum. The horizontal lines, $y^+ = 80$ and $y/h = 0.2$, represent conventional logarithmic layer limits. Diagonal is $\lambda_x = 5y$. Arrows indicate the implied cascades

flows, such as jets or mixing layers, this leads to a large-scale instability of the mean velocity profile [3], and to large-scale eddies with sizes of the order of the flow thickness.

The mean velocity profiles of wall-bounded flows are not unstable in the same way as the free-shear cases, and wall-bounded turbulence is consequently a weaker phenomenon. While the velocity fluctuations in a jet can easily reach 15-20% of the mean velocity differences, they rarely exceed 5% in attached boundary layers. Wall-bounded flows are however of huge technological importance. Roughly half of the energy spent worldwide to move fluids through pipes and canals, or to move vehicles through air or through water (20% of the total), is dissipated by turbulence in the immediate vicinity of the wall.

Wall-bounded flows are also interesting because they force us to face the role of inhomogeneity. This can be seen in figure 1(b) which is the equivalent of figure 1(a) for a wall-bounded turbulent flow. Each horizontal section of this figure is equivalent to the spectra in figure 1(a). The energy is again at large scales, while the dissipative eddies are smaller. In this case, however, the size of the energy-containing eddies changes with the distance to the wall, and so does the range of scales over which the energy has to cascade. The eddies containing most of the energy at one wall distance are in the midst of the inertial cascade when they are observed farther away from the wall. The Reynolds number, defined as the scale disparity between energy and dissipation at some given location, also changes with wall distance. The main emphasis in wall turbulence is not the inertial energy cascade, but the interplay between different scales at different distances from the wall.

Models for wall-bounded turbulence also have to deal with spatial fluxes that are not present in the homogeneous case. The most important ones are those of momentum. Consider a turbulent channel, driven by a pressure gradient between infinite parallel planes. Denote by U, V and W the mean velocities along the streamwise, wall-normal and spanwise directions, x, y and z, and the corresponding fluctuations by lower-case letters. Streamwise momentum is fed into the channel by the mean pressure gradient, $\partial_x P$, which acts over the whole cross section. It is removed only at the wall, by viscous friction. Momentum has to flow from the centre to the wall, carried by the Reynolds stress $-\langle uv \rangle$, which resides in eddies of roughly the same sizes as the energy, and it is clear from figure 1(b) that those sizes change as a function of the wall distance by as much as the scale of the energy across the inertial cascade. This implies that momentum is transferred in wall-bounded turbulence by an extra spatial 'cascade'. Momentum transport is present in all shear flows, but the multiscale spatial cascade is characteristic of very inhomogeneous situations, such as wall turbulence, and complicates the problem considerably.

In this paper we review what is known about the interactions of the different structures in wall-bounded flows. In section 2 we summarise the present conceptual models for both the viscous and the outer regions, and in section 3 we discuss briefly how the two regions interact with each other, and in particular the question of whether causality flows from the wall to the outside, or viceversa.

2 The General Organisation of Wall-Bounded Turbulence

The wall-normal variation of the range of the energy cascade divides the flow into several distinct regions. Wall-bounded turbulence over smooth walls has to be described by two sets of scaling parameters [39]. Viscosity is important near the wall, and the units for length and velocity in that region are constructed with the kinematic viscosity ν, and the friction velocity u_τ. Magnitudes expressed in wall units are denoted by $^+$ superscripts, and y^+ is a Reynolds number for the size of the structures. It is never large within the viscous layer, which is typically defined at most as $y^+ \lesssim 150$ [32], and conventionally divided into a viscous sublayer, $y^+ \lesssim 5$, where viscosity is dominant, and a 'buffer' layer in which both viscosity and inertial effects should be taken into account. There is no scale disparity in either region, as seen in figure 1(b), because most large eddies are excluded by the presence of the impermeable wall. The energy and the dissipation are at similar sizes.

Away from the wall the velocity also scales with u_τ, because the momentum equation requires that the Reynolds stress, $-\langle uv \rangle$, can only change slowly with y. This uniform velocity scale is the extra constraint introduced in wall-bounded flows by the momentum transfer. The lengthscale in the region far from the wall is the flow thickness h, which in this paper will usually be the semi-channel height.

Between the inner and the outer regions there is an intermediate layer where the only available lengthscale is the wall distance y. Both the constant velocity scale across the intermediate region, and the absence of a lengthscale other than y, are only approximations. It will be seen below that some large-scale eddies of size $O(h)$

penetrate to the wall, and that the velocity fluctuations do not scale strictly with u_τ, even in the viscous sublayer. However, if those approximations are accepted, the 'logarithmic' mean velocity profile,

$$U^+ = \kappa^{-1} \log y^+ + A, \tag{1}$$

follows from symmetry arguments. It agrees well with experimental evidence, with an approximately universal Kármán constant, $\kappa \approx 0.4$, and $A \approx 5$ for smooth walls.

The viscous, buffer, and logarithmic layers are the most characteristic features of wall-bounded flows, and constitute the main difference between them and other types of turbulence.

2.1 The Buffer Layer

The viscous and buffer layers, although generally very thin, are extremely important for the flow as a whole. The ratio between the inner and the outer lengthscales is the friction Reynolds number, h^+, which ranges from 200 for barely turbulent flows, to 5×10^5 for large water pipes. In the latter, the near-wall layer is only about 3×10^{-4} times the pipe radius, but it follows from equation (1) that, even in that case, 40% of the velocity drop takes place below $y^+ = 50$. Because there is relatively little net energy transfer among layers, except in the viscous region, those percentages also apply to the energy dissipation. Turbulence is characterised by the expulsion towards the small scales of the energy dissipation, away from the large energy-containing eddies. In the limit of infinite Reynolds number, this is believed to lead to a non-differentiable velocity field. In wall-bounded flows that separation occurs not only in the scale space for the velocity fluctuations, but also in the shape of the mean velocity profile. The singularities are expelled both from the large scales, and from the centre of the flow towards the walls.

The viscous layers are dominated by coherent streaks of the streamwise velocity and by quasi-streamwise vortices, which are both the energy-containing and the dissipative eddies. The streaks are an irregular array of long ($x^+ \approx 1000$) sinuous alternating streamwise jets superimposed on the mean shear, with an average spanwise separation of the order of $z^+ \approx 100$ [37]. The quasi-streamwise vortices are slightly tilted away from the wall, and stay in the near-wall region only for $x^+ \approx 200$. Several vortices are associated with each streak [23], with a longitudinal spacing of the order of $x^+ \approx 400$. Most of them merge into disorganised vorticity outside the immediate neighbourhood of the wall [36].

It was soon proposed that streaks and vortices are involved in a regeneration cycle in which the vortices are the results of an instability of the streaks [38], while the streaks are caused by the advection of the mean velocity gradient by the vortices [2, 26]. Both processes have been documented and sharpened by numerical experiments. For example, disturbing the streaks inhibits the formation of the vortices, but only if it is done between $y^+ \approx 10$ and $y^+ \approx 60$ [24], suggesting that it is predominantly between those two levels that the regeneration cycle works. There is substantial numerical and analytic work showing that streaks are linearly unstable

to sinuous perturbations associated with inflection points of the distorted velocity profile, whose eigenfunctions correspond well with the shape and location of the observed vortices. The implied model is a time-dependent cycle in which streaks and vortices are created, grow, generate each other, and eventually decay. Reference [24] discusses models of this type, and gives additional references.

Although the flow in the buffer layer is clearly chaotic, the chaos is not required to explain the turbulence statistics. Simulations in which the flow is substituted by an ordered 'crystal' of identical 'minimal' sets of structures reproduce fairly well the correct statistics [23]. In a further simplification, that occurred at roughly the same time as the previous one, nonlinear equilibrium solutions of the three-dimensional Navier–Stokes equations were obtained numerically in Couette flow, with characteristics that suggested that they could be useful in a dynamical description of the near-wall region [31]. Many similar solutions were soon found in other wall-bounded flows, including limit cycles and heteroclinic connections reminiscent of the cycle mentioned above. All of them look qualitatively similar [41, 22], and take the form of a wavy low-velocity streak flanked by a pair of staggered quasi-streamwise vortices of alternating signs, closely resembling the spatially-coherent objects educed from the near-wall region of true turbulence.

Those solutions were recently reviewed and extended in [22]. It turns out that they can be classified into 'upper' and 'lower' branches in terms of their mean wall shear. The 'upper' solutions have relatively weak sinuous streaks flanked by strong vortices. They consequently have relatively weak streamwise-velocity fluctuations, and strong wall-normal ones, at least when compared to those in the lower branch. Their mean and fluctuating velocities are reminiscent of experimental turbulence [25, 42], and so are other properties. For example, the range of spanwise wavelengths in which the nonlinear solutions exist is in the neighbourhood of the observed spacing of the streaks of the sublayer [22]. 'Lower' solutions have stronger and essentially straight streaks, and much weaker vortices. Their statistics are very different from turbulence.

The near-wall statistics of full turbulent flows, when compiled over scales corresponding to a single streak and to a single vortex pair, are independent of the Reynolds number, and agree reasonably well with those of the fixed points, although there is a noticeable contribution from unsteady bursting [22]. When they are compiled over much larger boxes, however, the intensity of the fluctuations does not scale well in wall units, even very near the wall [7]. That effect is due to large outer-flow velocity fluctuations reaching the wall, and is unrelated to the structures being considered here.

This is shown in figure 2(a), which contains two-dimensional spectral energy densities of the streamwise velocity in the buffer layer, $k_x k_z E_{uu}(k_x, k_z)$, displayed as functions of the streamwise and spanwise wavelengths. The three spectra in the figure correspond to turbulent channels at different Reynolds numbers. They differ from each other almost exclusively in the long and wide structures represented in the upper-right corner of the spectrum, whose sizes are of the order of $\lambda_x \times \lambda_z = 10h \times h$ [8, 21, 17]. The lower-left corner of the spectral plane contains the structures discussed in this section, which are very approximately universal and local to the

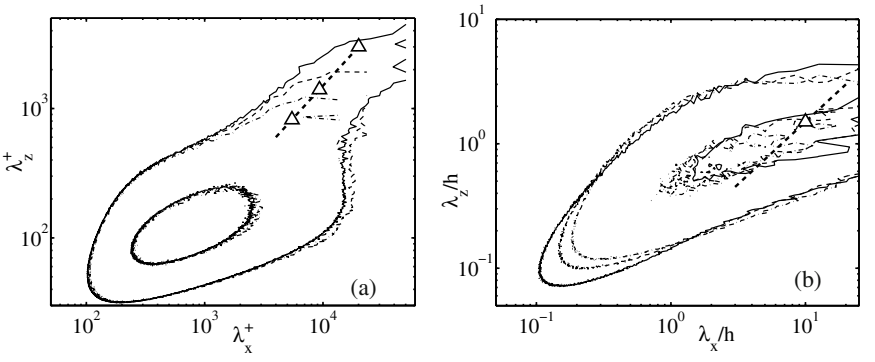

Fig. 2 Two-dimensional spectral energy density of the streamwise velocity, in terms of the streamwise and spanwise wavelengths. (a) $y^+ = 15$. (b) $y/h = 0.2$. Numerical channels [8, 11, 17]. —·— , $h^+ = 547$; – – – – , 934; ——— , 2003. Spectra are normalised in wall units, and the two contours for each spectrum are 0.11 and 0.55 times the maximum of the spectrum for the highest Reynolds number. The heavy diagonal is $\lambda_z = 0.15\lambda_x$, and the triangles are $\lambda_x = 10h$ for the three cases

near-wall layer. The larger structures in the top-right corner extend into the logarithmic layer, scale in outer units, and correspond approximately to Townsend's 'attached eddies' [40]. An example of their spectra away from the wall is shown in figure 2(b).

2.2 The Logarithmic Layer

The logarithmic layer is located just above the viscous region, and it is also unique to wall turbulence. Most of the velocity difference that does not reside in the near-wall region is concentrated in the logarithmic layer, which extends experimentally up to $y \approx 0.2h$ (figure 1b). It follows from the profile in (1) that the velocity difference above the logarithmic layer is only 20% of the total when $h^+ = 200$, and decreases logarithmically as the Reynolds number increases. In the limit of infinite Reynolds number, all the velocity drop is in the logarithmic layer.

This layer is an intrinsically high-Reynolds number phenomenon, which requires at least that its upper limit should be above the lower one, so that $0.2h^+ \gtrsim 150$, and $h^+ \gtrsim 750$. It has been studied experimentally for a long time, but numerical simulations with even an incipient logarithmic region have only recently become available [11, 17, 13]. It is much worse understood than the viscous layers, but the new simulations, together with simultaneous advances in experimental methods, have greatly improved our knowledge of the kinematics of the structures in this region, and are beginning to hint at models for their dynamics.

It is important to note at this point that the meaning of the word 'model' is probably different in the logarithmic and in the buffer layers. Near the wall, the local Reynolds numbers are low, and the structures are smooth and essentially analytic. It is then possible to speak of 'objects', and to write differential equations for their

behaviour. Above the buffer layer both things are harder to do. Since the definition of the outer layer includes $y^+ \gg 1$, its largest structures have high internal Reynolds numbers, and are turbulent themselves. There is presumably a cascade connecting those energy-containing structures with the dissipative scales, and their velocity fields can be expected to have nontrivial algebraic spectra and non-smooth geometries that can only be described statistically. They are 'eddies', rather than 'vortices', because turbulent vorticity always resides at the viscous Kolmogorov lengthscale η, separated from the energy-containing eddies by a scale ratio $O(y^{+3/4})$.

While the models for the buffer layer are in the realm of direct numerical simulations (DNS), the outer layers are the domain of large-eddy simulations (LES). This of course does not mean that the logarithmic layer can not be DNSed, and it is almost certain that more direct simulations will be required before this part of the flow is understood, but we can probably only expect simple models for partial aspects of the structures involved, rather than full ones including all the flow scales.

The first new information provided by the numerics on the logarithmic layer was spectral. It had been found experimentally that there are very large scales in the outer regions of turbulent boundary layers [19, 27], and DNS provided information about their two-dimensional spectra, and about their wall-normal correlations [8, 11]. The longest scales are associated with the streamwise velocity component. Its spectral density in the logarithmic layer has an elongated shape along the line $\lambda_z^2 = y\lambda_x$, while the two other velocity components are more isotropic. When three-dimensional flow fields became available, it was found that there is a self-similar hierarchy of compact ejections extending from the outer flow into the buffer layer, within which the coarse-grained dissipation is more intense than elsewhere [12]. They correspond to the isotropic spectra of the wall-normal velocity. When the flow is conditionally averaged around them, they are associated with long, conical, low-velocity regions in the logarithmic layer [12], whose intersection with a y-plane is parabolic, explaining the quadratic behaviour of the spectrum of u. These structures are not only statistical constructs. Individual cones are observed as low-momentum 'ramps' in streamwise sections of instantaneous flow fields [29].

When the cones reach heights of the order of the flow thickness, they stop growing, and become cylindrical 'streaks' spanning the distance from the central plane to the wall [8, 11], similar to those of the sublayer, but with spanwise scales of $2-3h$. They are fully turbulent objects. Neither in simulations nor in experiments in channels or pipes has it been possible to determine the maximum length of those 'global modes', which appear in any case to be longer than $25h$ [11, 18]. There is however some evidence that they may be shorter in boundary layers. The overall arrangement of the ejections and cones is reminiscent of the association of vortices and streaks in the buffer layer, but at a much larger scale. Their near-wall footprints are seen in the spectra of the buffer layer as the 'tails' in figure 2, and account [17] for the experimentally-observed Reynolds number dependence of the intensity of the near-wall velocity fluctuations [7].

Since we saw above that the sublayer streaks originate from the advection of the mean shear by cross-stream perturbations, which is a linear process, there is some hope that a linear model could also capture the formation of the outer-layer streaks.

The mean velocity profile of turbulent channels is linearly stable [34], but it has been known for some time that even stable flows can lead to large transient energy amplifications, because the evolution operator of the linearised Navier–Stokes equations is not self-adjoint [15, 4]. Simple linearised analysis of a uniform shear shows that the long-time asymptotic state of any localised perturbation is a u-streak, but it provides no wavelength-selection mechanism. When the analysis is repeated for nontrivial profiles, such as laminar or turbulent channels, the flow thickness provides a lengthscale and a wall-normal modal structure. The key modelling assumption to obtain structures mimicking the turbulent eddies of the logarithmic and outer regions appears to be the use of a y-dependent eddy viscosity similar to that required to maintain the experimental mean profile [33, 9]. Note that this implies that the resulting model applies to averaged eddies, rather than to individual structures. It turns out that there are two sets of wavelengths for which the total energy is most amplified, with eigenfunctions peaking at the two locations where the viscosity does not depend on y. Near the wall, where the viscosity is mostly molecular, they have spanwise wavelengths and eigenfunctions similar to the observed sublayer streaks. Near the central plane, where $\nu_T \approx u_\tau h$ is also roughly uniform, they are large-scale streaks with spanwise wavelengths of the order of the observed $3h$, and wall-normal eigenfunctions that agree well with the dominant proper orthogonal decomposition eigenmodes of the streamwise velocity at those wavelengths.

3 The Direction of Causality

We know less about how the ejections are created, but linear analysis also gives some information on them. In the same way as the linear effect of transverse perturbations is to create transient u-streaks, any perturbation of u that is not infinitely long transfers energy into the transverse velocity components. The same transient-growth analysis giving the large-scale streaks contains nontrivial amplifications for v and w, which could in principle feed a linear cycle in which v ejections create streaks by extracting energy from the mean shear, while the streaks in turn create ejections. Unfortunately the wavelengths of both processes are different, which is why the profile is linearly stable. The most amplified u-structures are streaks elongated along x, while the most amplified v and w are roughly isotropic in the wall-parallel plane. This agrees with the spectral evidence, but means that nonlinearity is required to match the wavelengths, and to close the cycle. It is however easy to visualise a process by which an ejection creates a strong streak, whose enveloping shear layer becomes unstable and creates new, shorter ejections. In fact, we have seen that compact ejections can be identified at all scales in the logarithmic and outer layers, both numerically and experimentally, and that they are associated with streaks. It is known, from the analysis of their relative lengths and lifetimes, that the observed ejections cannot be the origin of the full length of the streak to which they are associated, and that some causal link from streaks to ejections is also required [9]. In fact, numerical experiments with 'minimal' simulation boxes of the order of the channel width, several thousand wall units long and wide, show evidence of an 'outer' cycle

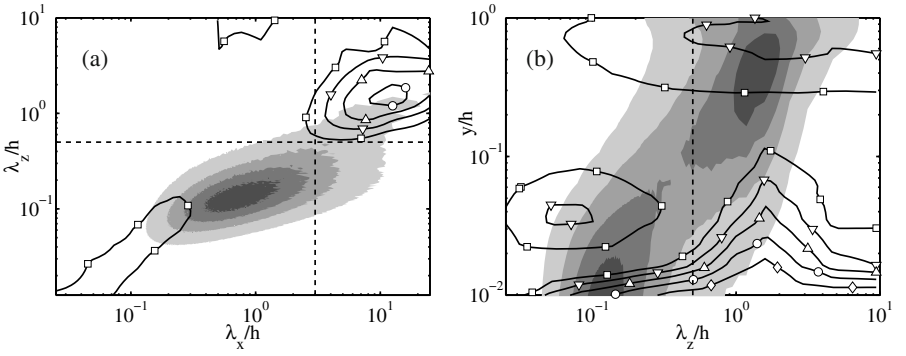

Fig. 3 Contour plot of the coherence coefficient of the streamwise velocity fluctuations. Numerical channel at $Re_\tau = 934$ [11]. (a) As a function of both wavelengths at $y^+ = 20$. (b) Maximum over λ_z, as a function of the λ_x and y. The isolines are, $\square$ –$\diamondsuit$, $\gamma = 0.25(0.1)0.65$. The shaded contours are the premultiplied energy density of the streamwise velocity, normalised at each wall distance with the fluctuation energy. The horizontal or vertical dashed lines correspond to $\lambda_z = 0.5h$ and $\lambda_x = 3h$

of the largest flow scales, with a characteristic period ($tu_\tau/h \approx 2.5$, $t^+ \approx 4500$), that appears to be unrelated to any near-wall process [14].

There is clear evidence that this outer structures are coherent, and influence the wall. Figure 3 shows the correlation coefficient between the temporal and spatial derivatives of u,

$$\gamma_u = \frac{\langle \partial_t u \, \partial_x u \rangle}{[\langle (\partial_t u)^2 \rangle \langle (\partial_x u)^2 \rangle]^{1/2}}, \tag{2}$$

which measures how far is the velocity field from being a coherent wave [10]. Figure 3(a) shows that the only wave-like behaviour in the buffer layer corresponds to structures that are much larger than the local turbulent cycle, while 3(b) shows that they are reflections of structures residing near the centre of the channel.

The outer structures clearly modify the inner layer, although most of the modification is probably trivial. It is clear from figure 3 that the sizes of both sets of structures are very different. Even at the relatively modest Reynolds number of the figure the scale ratio is roughly 20, and it increases linearly with the Reynolds number. The near-wall streaks effectively live in a local boundary layer whose friction velocity and mean flow direction is defined by the outer structures. For example, one could think of the local atmospheric surface layer, in which streaks with lengths of centimetres live within drafts several hundred meters long. When this effect is discounted, most of the effect of the Reynolds number disappears. For example, it was shown in [22] that, when the velocity fluctuation intensities are computed over local boxes of the size of a minimal flow unit, with respect to the local mean and normalised with the local friction velocity, their probability density functions become independent of the Reynolds number. The same is true for larger averaging boxes, as long as their sizes are scaled in wall units. The direct relation between higher